JOURNAL OF
Bioactive and Compatible Polymers

Original Article

Journal of Bioactive and Compatible Polymers
2016, Vol. 31(2) 208–224

DOI: 10.1177/0883911515602709
jbc.sagepub.com
SAGE

Electrospun silk fibroin–poly (lactic-co-glycolic acid) membrane for nerve tissue engineering

Jianchao Zhan[1,2], Junyi Liu[1], Chunyang Wang[3], Cunyi Fan[3], Hany A El-Hamshary[4,5], Salem S Al-Deyab[4] and Xiumei Mo[1,4]

Abstract

Silk fibroin–poly(lactic-co-glycolic acid) fibrous membranes were electrospun by varying the weight ratios for silk fibroin to poly(lactic-co-glycolic acid). The hydrophilicity, mechanical property, and biodegradability of the fibrous in vitro were evaluated. Contact angle test demonstrated that the hydrophilicity of poly(lactic-co-glycolic acid) fibrous membrane could be improved by introducing silk fibroin ingredient. Mechanical test showed that the strain–elongation performances of silk fibroin–poly(lactic-co-glycolic acid) fibrous can be controlled by changing the silk fibroin percentage. 3-(4,5-Dimethylthiazol-2-yl)-5-(3-carboxymethoxyphenyl)-2-(4-sulfophenyl)-2H-tetrazolium assay test showed that the silk fibroin–poly(lactic-co-glycolic acid) 2:8 fibrous enhanced the nerve cell proliferation compared to poly(lactic-co-glycolic acid) fibrous. Silk fibroin–poly(lactic-co-glycolic acid) fibrous membrane has been made into the nerve guidance conduit by the reeling and the sewing processing. The poly(lactic-co-glycolic acid) nerve guidance conduit and silk fibroin–poly(lactic-co-glycolic acid) nerve guidance conduit were implanted into a 10-mm sciatic nerve defect part of mice for nerve regeneration and the nerve regenerated at 12 weeks. Nerve regeneration test showed that the regenerated nerve in the silk fibroin–poly(lactic-co-glycolic acid) nerve guidance conduit group was more organized and mature than that in the poly(lactic-co-glycolic acid) nerve guidance conduit group. The results suggest that the silk fibroin–poly(lactic-co-glycolic acid) (2:8) nerve guidance conduits have potential applications in nerve regeneration.

[1]State Key Laboratory for Modification of Chemical Fibers and Polymer Materials, College of Chemistry, Chemical Engineering and Biotechnology, Donghua University, Shanghai, China
[2]College of Materials and Textile Engineering, Jiaxing University, Jiaxing, China
[3]Department of Orthopedic Surgery, Shanghai Sixth People's Hospital, Shanghai Jiao Tong University, Shanghai, China
[4]Department of Chemistry, College of Science, King Saud University, Riyadh, Kingdom of Saudi Arabia
[5]Department of Chemistry, Faculty of Science, Tanta University, Tanta, Egypt

Corresponding author:
Xiumei Mo, State Key Laboratory for Modification of Chemical Fibers and Polymer Materials, College of Chemistry, Chemical Engineering and Biotechnology, Donghua University, Shanghai 201620, China.
Email: xmm@dhu.edu.cn

Keywords
Electrospun nanofibers, tissue engineering scaffold, nerve guidance conduit, poly(lactic-co-glycolic acid), silk fibroin

Introduction

Peripheral nerve injuries often lead to some patients permanently disabled, which brings huge economic loss and mental burden to the patients, their family, and even the whole society. Hence, how to promote nerve regeneration and restore the function of target organs has always been the hotspot of the attention. As for the peripheral nerve break, the separated nerves are linked by suture to restore nerve continuity after axotomy. As to peripheral nerve defects, an autologous nerve graft is still the clinical "gold standard" for surgical repair. However, there are some problems difficult to be solved, such as low speed of regeneration, limited autograft nerve source, and the mismatch between the donor and the receptor; at the same time, cut autologous nerve will lead to injury and dysfunction of the donor area. Therefore, looking for a substitute for autologous nerve has become a research hotspot.

In recent years, with the rise in tissue engineering, it brought the dawn to the patients with tissue defects or organ failure.[1] Nerve regeneration conduit constructed using biological material not only provides a favorable space for nerve cells to get nutrition, growth, and metabolism but also guides the growth of nerve fibers.

There are many research reports about nerve conduit; it can be divided into single-channel conduits and multi-channel conduits, or added to guide fibers in the conduits.[2–5] Fan et al.[6] prepared chitosan single-channel nerve conduit which had been successfully used in a 35-mm-long peripheral nerve injury repair. Ao et al.[7] developed chitosan nerve conduit via freeze-drying method. Many studies show that the nanofiber tissue repair materials can significantly promote cell adhesion, growth, and differentiation; regulate the intracellular signal path of control transcriptional activity and gene expression; and guide the orientation of cytoskeletal proteins. The larger surface area of the nanoscale scaffold (such as nanofiber membrane) is conductive to absorb more protein and provides more adhesion sites on the cell membrane receptor, and the adsorbed protein can also be exposed to more hidden adhesion sites through a conformational change, thus good for cell adhesion.[8] In addition, through contact guidance mechanism, aligned fibrous topology is able to control the growth of nerve cells, promote axonal stretch, and grow along the direction of the fibers.[9–11]

Electrospinning fiber has also been widely applied in neural tissue engineering.[12,13] Our research group has prepared silk fibroin (SF)–poly (L-lactic acid-co-ε-caprolactone) composite fibrous nerve conduits by electrospinning, and it has been successfully used for a 10-mm-long sciatic nerve injury repair.[14] It has been found that tubular nerve conduits fabricated by electrospinning possess good mechanical properties and suture performance, in addition, which can also mimic the structure of the extracellular matrix.

Cocoon silk constitutes 75% of SF and 25% of silk sericin. As natural protein, SF has several attractive properties, including abundant resources, biodegradation, and good biocompatibility.[15–18] Gu's research group obtained the SF fibers co-cultured with Schwann cells (SCs) which were extracted from the rat central nervous and sciatic nerve, and they found that SF scaffolds can promote peripheral nerve regeneration close to the autologous nerve grafts.[19,20] In conclusion, SF can promote peripheral nerve repair. However, the electrospun SF nanofiber membrane is brittle with lower tensile strength and elongation at break.[21–23] Poly(lactide-co-glycolide) (PLGA) as a synthetic polymer biomaterials has been widely used in the tissue engineering.[24] The electrospun PLGA fibrous owns the appropriate degradation rate and mechanical behavior and has been identified as a

potential candidate of nerve guidance conduits (NGCs).[25] To overcome the brittleness of SF, we blended PLGA with SF to fabricate SF-PLGA fibrous membranes and SF-PLGA NGCs and regarded the properties of which in vitro and in vivo. In this study, we aimed to investigate the SCs' growth behavior into SF-PLGA fibrous membranes and evaluated the characteristics of the regenerated nerve when the SF-PLGA NGCs bridged the nerve defect.

Experimental methods

Materials

PLGA (molecular weight (Mw) = 100,000, Lactic Acid/ Glycolic Acid (LA/GA) = 75/25) was obtained from Jinan Daigang Biomaterial Co., Ltd (China). Mulberry silkworm cocoon was supplied by Jiaxing Silk Co., Ltd (China). Hexafluoroisopropanol (HFIP) was obtained from Shanghai Chem Co., Ltd (China). Dulbecco's Modified Eagle Medium (DMEM), fetal bovine serum (FBS), and trypsin were obtained from Hangzhou Jinuo Biomaterial Co., Ltd (China). Penicillin and streptomycin were purchased from Shanghai Generay Biotech Co., Ltd. Phosphate buffer solution (PBS) was obtained from Sigma (USA).

Preparation of SF

SF was prepared according to the method previously described by Zhang et al.[21–23] In brief, raw silk was boiled in 0.5% (w/w) Na_2CO_3 solution and then rinsed thoroughly with distilled water to remove sericin. The degummed silk was dissolved in a $CaCl_2/H_2O/C_2H_5OH$ (1/8/2 mole ratio) solution at 70°C for 6 h. After dialysis with cellulose tubular membrane (250-7u; Sigma) in distilled water for 3 days, the silk solution was freeze-dried to obtain regenerated SF.

Preparation of SF-PLGA fibrous membrane and NGCs

The 12 wt% SF-PLGA-blended solution with the SF:PLGA weight blending ratios of 8:2, 5:5, 2:8, and 0:10 was prepared. The SF-PLGA solution was filled in a syringe equipped with a blunt 7 gauge needle and the solution was pump out with flow rate of 0.8 mL/h for electrospinning when a supply voltage (20 kV) was applied to the needle. SF-PLGA fibrous was collected on a rotating drum (diameter: 5 cm) with a rotating speed of 500 r/min. The distance between the drum and needle tip was set at 14 cm. In addition, SF fibrous was successfully fabricated at the concentration of 18% (g/mL, using HFIP as solvent) via electrospinning. The fibrous was dried overnight in a dessicator and then was treated with methanol vapor for 6 h. NGC was prepared according to the method previously described by Wang et al.[14] The fibrous membrane was rolled into a tube which was sutured with sewing thread to give the NGC (Figure 1).

Surface characterization of electrospun fibrous membranes

The morphology of the fibrous was observed under scanning electron microscopy (SEM; JSM-5600LV, Japan) after the surface of the fibrous was sputter-coated with gold. The average diameter of the fibrous (n = 100) was measured using SEM-assisted image analysis software.

Mechanical testing

The test equipments used were a universal material tester H5K-S (Hounsfield, UK) and a digital micrometer. The test conditions are as follows: 20°C and 65% relative humidity (RH). The sample

Figure 1. Exterior contour of the NGC (length = 12 mm, inner diameter = 1.4 mm, wall thickness = 0.3 mm).

preparation was as follows: length (50 mm) × width (10 mm) × thickness (random test). The ultimate strength and tensile elongation were calculated by the following equations

$$\text{Ultimate strength (MPa)} = \frac{\text{break force (N)}}{\text{thickness (mm)} \times \text{width (mm)}}$$

$$\text{Tensile elongation (\%)} = \frac{\text{absolute elongation (mm)}}{\text{guage length (mm)}} \times 100\%$$

Hydrophilicity measurements

Hydrophilicity of the fibrous membrane was measured by contact angle instrument (OCA40; DataPhysics, Germany). Distilled water was automatically dropped onto the fibrous membrane and the contact angle was calculated automatically.

Degradation testing

The electrospun fibrous membrane was cut into rectangles ($3 \times 6\,cm^2$) and immersed in the PBS (pH 7.4, 20 mL PBS each sample) at 37 ± 0.1°C. Sodium azide (2 mg/mL) was put into the PBS solution. The incubation vessels were shaken in a shaking incubator and the incubating media were exchanged every 2 weeks. At each predetermined time point, the samples were freeze-dried and then were weighted. The weight loss rate (WLR) was calculated by the following equation

$$\text{WLR} = \frac{w_b - w_f}{w_b} \times 100\%$$

where WLR is the WLR of the fibrous, w_b is the initial weight, and w_f is the dry weight after degradation.

Biological evaluation

Cell seeding. Prior to cell seeding, all fibrous membranes were sterilized for 4 h with the use of ethanol solution (75%, v/v). The sterilized membrane was rinsed in PBS solution and then in culture

medium. Membranes were put onto coverslips, which were then put into 24-well tissue culture plate (one sample per well). Rat SCs were seeded onto the samples at a density of 1.0×10^4 cells per well in DMEM supplemented with 10% FBS and incubated at 37°C and 95% RH, in a 5% CO_2 incubator.

Cell viability. At each predetermined time point, the cell-seeded membrane was immersed into the 3-(4,5-dimethylthiazol-2-yl)-2,5-diphenyltetrazolium bromide (MTT) solution (5 mg/mL MTT in cell culture medium) for 4 h in the incubator (37°C, 5% CO_2) and formed the purple formazan reaction product. The dimethyl sulfoxide (DMSO, 400 μL) was added to the purple sediment and vibrated slightly for 20 min, and then the dissolved solution (100 μL) was transferred to a 96-well plate and the absorbance at 570 nm was measured using a Thermo Multiskan MK3.

In vivo nerve regeneration studies

Animal experiments. All animal experimental procedures were performed as per Institutional Animal Care guidelines and approved ethically by the Administration Committee on Experimental Animals, Shanghai, China. Adult male Sprague–Dawley rats (200–250 g) were randomly divided into three groups of 12 animals each: the PLGA NGC group, SF-PLGA NGC group, and autograft group. Ketamine was intraperitoneally injected into the experimental rats (100 mg/kg) and then the dorsolateral gluteal muscle was incised before the right sciatic nerve was exposed. Nerve segment (10 mm) was resected and then the NGCs bridged the nerve defect which was sutured to nerve stumps with 8-0 nylon sutures. All animals were housed and fed routinely after surgery.

Functional evaluation of regenerated nerves. Twelve weeks after surgery, the regenerated nerve at the injured side was exposed under anesthesia. Nerve conduction velocity (NCV) and compound motor action potential (CMAP) were recorded in the electrophysiological evaluation. Electrical activity of the sciatic nerve was induced by a monopolar recording electrode and bipolar stimulating electrodes corresponding to NCV and CMAP were recorded by a digital MYTO electromyographic machine (Italy, Esaote).

Morphological analysis of regenerated nerves. Twelve weeks after nerve grafting, the NGCs were carefully removed and the regenerated nerve was exposed. Using toluidine blue staining and transmission electron microscopy (TEM), the axonal in the middle of the regenerated nerve was investigated. The samples were fixed, cut into thin sections (1 μm) at the middle segment of the regenerated nerve, and stained according to the method previously described by Wang et al.[14] The number of nerve fiber, the thickness of the myelin sheath, and percent neural tissue were calculated using Image J software.

Results and discussion

Morphology of fibrous membrane

The morphology of the membrane was observed under SEM and the average diameter of the fiber (n = 100) was measured using SEM-assisted image analysis software (Figure 2). It can be observed that the surface of the fiber is smooth. The mean fiber diameters are 911 ± 403, 379 ± 217, 386 ± 145, 527 ± 237, and 725 ± 380 nm, corresponding to the weight ratio for SF to PLGA of 10:0, 8:2, 5:5, 2:8, and 0:10, respectively. The mean diameters of pure SF fiber are largest among them because SF fibers were electrospun at higher concentration (18 wt%; Figure 2(a)). At lower concentration of 12 wt%, the diameter of the fiber decreased with the increase in SF in the SF-PLGA fibrous

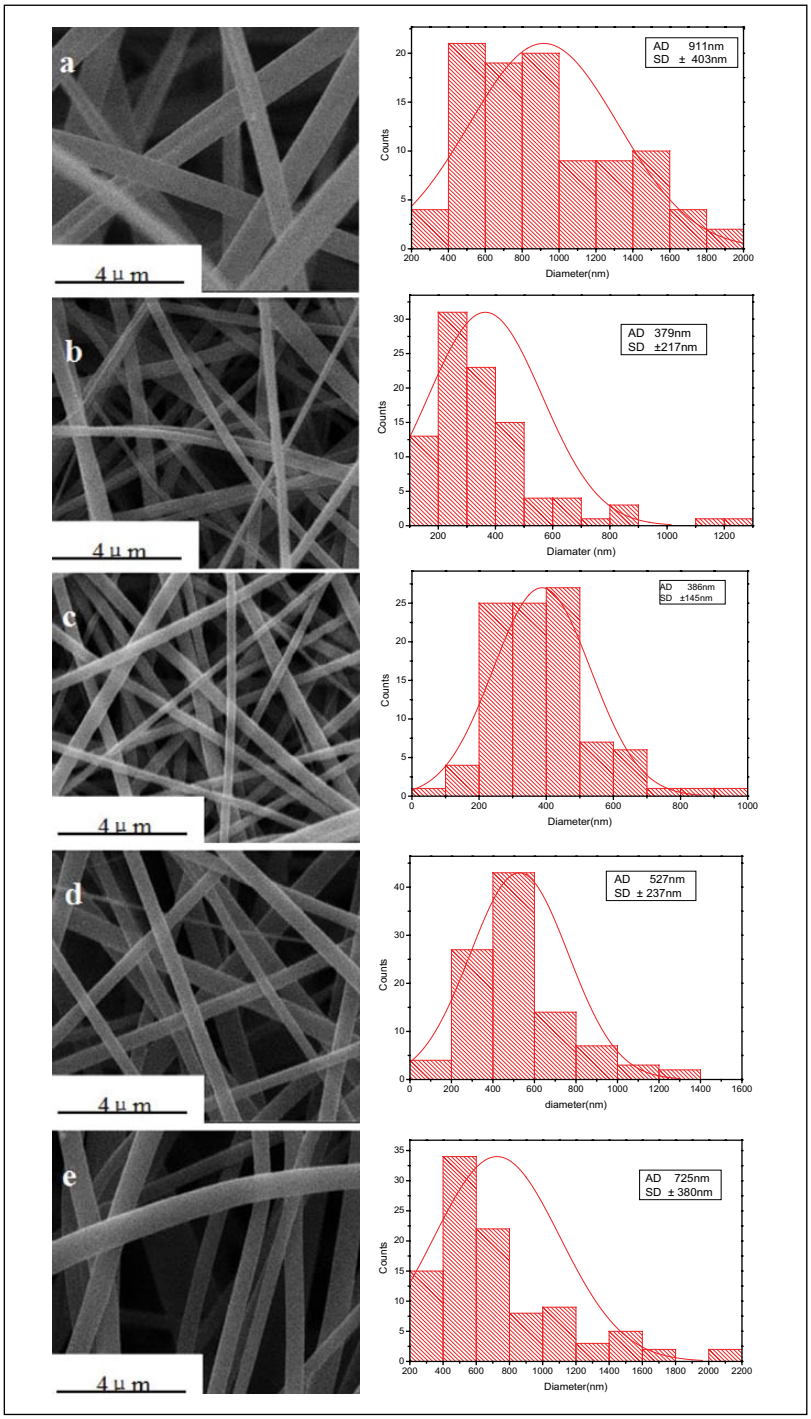

Figure 2. The left side are the SEM images of SF-PLGA fibrous membrane made at different weight ratios: (a) 10:0, (b) 8:2, (c) 5:5, (d) 2:8, and (e) 0:10; the right side is the corresponding diameter and distribution.

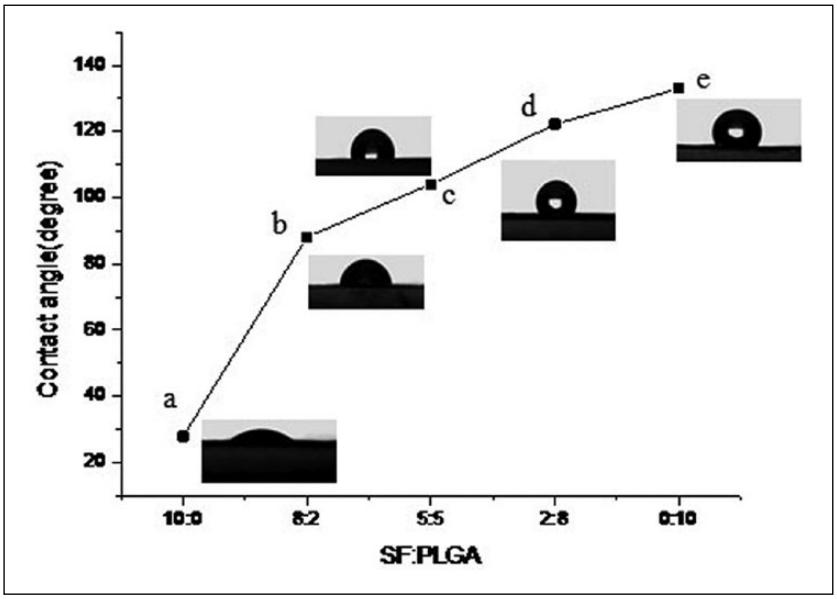

Figure 3. Water contact angle of SF-PLGA fibrous membrane with different weight ratios: (a) 10:0, (b) 8:2, (c) 5:5, (d) 2:8, and (e) 0:10.

(Figure 2(b) to (e)). A similar result was reported where the fiber diameter was found to decrease with the increase in weight ratio of silk and collagen.[26]

Wettability of SF-PLGA fibrous membrane

The wettability of the biomaterials has an important influence on the cell attachment, proliferation, and migration.[23] Because SF contains a large number of hydrophilic groups, the SF fibrous membrane showed high hydrophilicity. The average contact angle of pure PLGA fibrous membrane is around 133°, which indicates that PLGA fibrous membranes were hydrophobic. With increasing weight ratio of SF from 2 to 10, the contact angle of the fibrous decreased from 112.2° to 27.9° (Figure 3). The hydrophilicity of PLGA fibrous membrane could be improved by introducing SF ingredient.

Mechanical properties

Scaffolds for tissue engineering require appropriate mechanical property to guide tissue regeneration and facilitate implant operation. Figure 4 shows the tensile stress–strain curves of the electrospun SF-PLGA fibrous membrane. It can be observed that with the increase in SF content, the tensile stress and elongation at break of fibrous membrane decreased, which was similar to the relevant report.[27] The mechanical properties of SF-PLGA fibrous membrane became weak with the introduction of the SF, which suggests that the strain–elongation performances of SF-PLGA fibrous membrane can be controlled by changing the SF percentage. PLGA fibrous membrane demonstrated the advantageous mechanical property and the SF-PLGA fibrous membrane with 20% SF content showed the acceptable mechanical properties as an NGC.

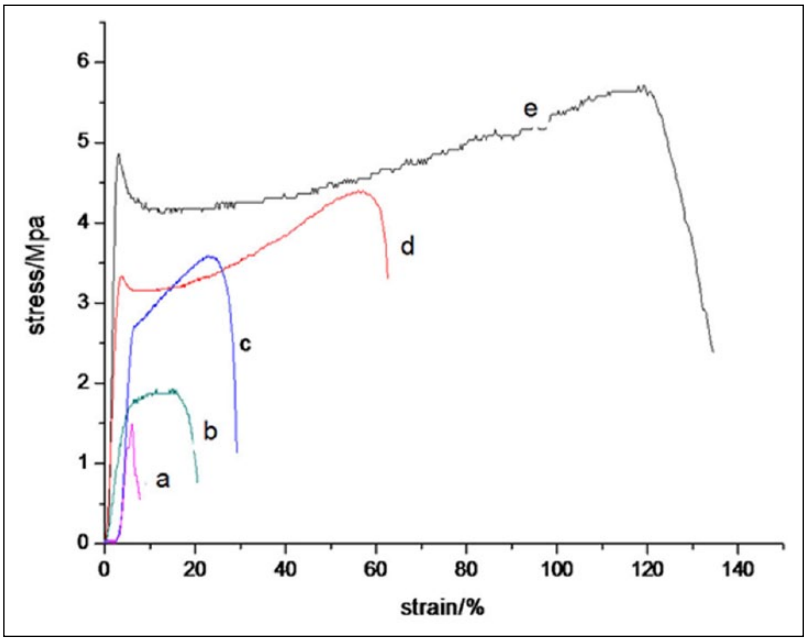

Figure 4. The strain and stress curves of the electrospun SF-PLGA fibrous membrane with the weight ratio of SF to PLGA: (a) 10:0, (b) 8:2, (c) 5:5, (d) 2:8, and (e) 0:10.

In vitro degradation of the SF-PLGA fibrous membrane

The biodegradability of NGCs plays an important role in guiding nerve regeneration. The ideal degradation rate of NGCs should be consistent with the rate of nerve regeneration.[28,29] Figure 5 shows the degradation curve of electrospun fibrous membrane when incubated in PBS for different times. It can be observed that the WLR of pure SF fibrous membrane was 2.6% after degradation for 12 weeks. The β-sheet crystal structure in SF prevented water penetrating to the inner side of the fiber, which reduced the hydrolysis degradation. In addition, peptide bond was difficult to fracture in neutral medium, which blocked the hydrolysis of protein.[30]

The WLR of pure PLGA fibrous membrane was 27.6% and the degradation rate was faster than that of pure SF fibrous membrane. The possible explanation is that the crystallinity of PLGA fibrous is lower than that of SF fibrous. The GA-GA or GA-LA linkage in the PLGA molecular chain is easy to be hydrolyzed, which speed up the degradation of PLGA.[24,31–33]

As to the SF-PLGA (2:8) fibrous membrane, the WLR was 50.2% and the degradation rate was the fastest one. A possible explanation is that with the addition of SF, the crystalline structure of the PLGA fiber was damaged, which favored the penetration of water molecules into the fibers and then speeded up the degradation.

The WLR of SF-PLGA (8:2) fibrous membrane was mainly due to the degradation of PLGA composition in the first 8 weeks. With the addition of SF, the crystalline structure of the PLGA fiber was damaged and the water molecule more easily entered into the fiber and then speeded up the degradation. So the degradation rate of SF-PLGA (8:2) membrane was faster than that of PLGA membrane in the first 8 weeks. After 8 weeks, the WLR of SF-PLGA (8:2) fibrous membrane was mainly due to the degradation of SF composition, which was lower than that of PLGA fibrous membrane.

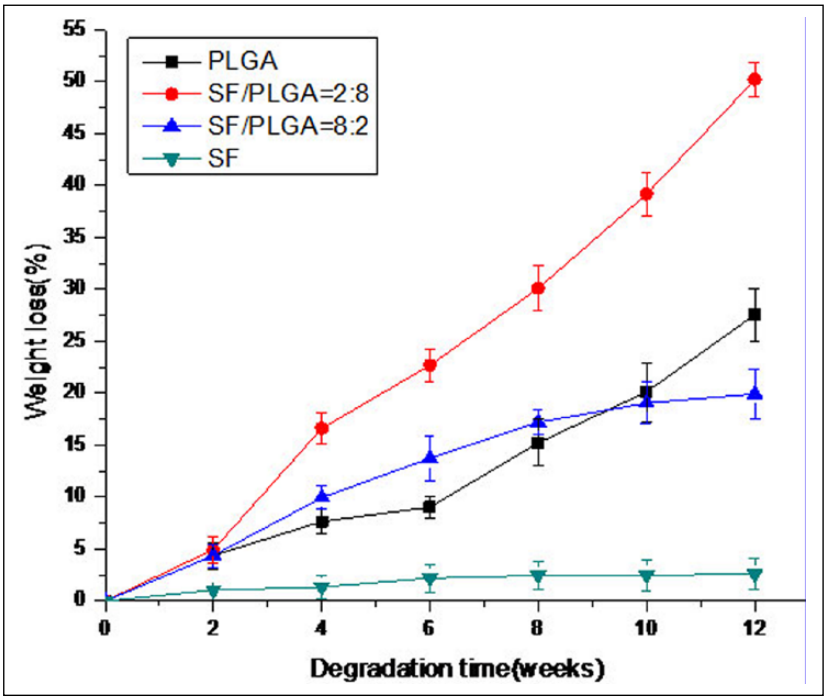

Figure 5. Weight loss of the SF-PLGA fibrous membrane during the process of degradation.

Cytotoxicity evaluation

As for the main structural and functional cells of peripheral nerve, SCs play an important role in nerve regeneration.[26] Therefore, we have evaluated the viability of SCs cultured in the SF-PLGA fibrous membrane. Figure 6 shows that the viability of SCs cultured on all membranes was significantly higher than that in coverslips at all time points after seeding ($*p < 0.05$; $**p < 0.01$). On Days 1 and 3, there was no significant difference ($p > 0.05$) in cell viability on SF-PLGA fibrous membrane, but on Days 5 and 7, the viability of cells on SF-PLGA fiber membrane was significantly higher than pure PLGA or SF fibrous membrane, indicating that the SF-PLGA fibrous has accelerated the viability of SCs, especially for SF-PLGA (2:8) fibrous membrane which showed the highest cell viability ($*p < 0.05$; $**p < 0.01$). Similar results reported that the viability of Pig iliac artery endothelial cells (PIECs) on SF-P(LLA-CL) (25:75) fibrous membrane was significantly higher than that of the SF-poly (L-lactic acid-co-ε-caprolactone) P(LLA-CL) (100:0, 75:25, 50:50, 0:100) groups,[21] which is the same as SF–hydroxybutyl chitosan fibrous membrane.[23] Alberto's research group has pointed out that the scaffolds were beneficial to the cell proliferation, differentiation, and function if the content of hydrophilic components is at around 20%.[34] The fiber diameter expanded after absorbing culture medium, which made the pore smaller and even damaged the nanostructures of SF-PLGA (10:0, 8:2, 5:5) fibrous membrane. PLGA fibrous membrane is unfavorable for the adhesion of SCs because of its hydrophobic surface. Therefore, the hydrophilic/hydrophobic balance of the SF-PLGA (2:8) fibrous membrane is important for the cell attachment activity[35] and which are potential substrates for nerve tissue engineering.

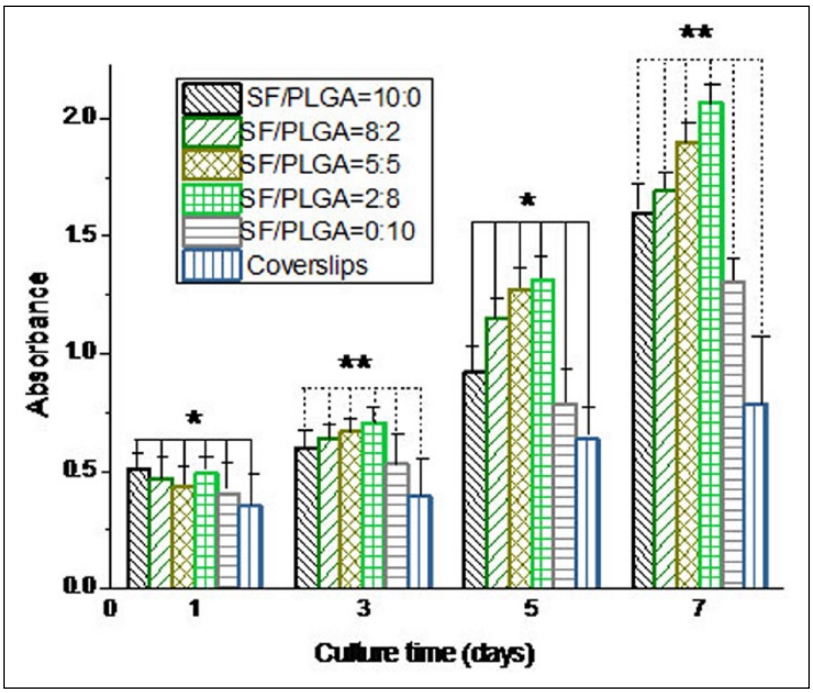

Figure 6. Schwann cells' viability on the electrospun SF-PLGA fibrous membrane and coverslips ($n = 4$; $^{*}p < 0.05$, $^{**}p < 0.01$).

NGC implantation and nerve regeneration

Figure 7 shows the contour of the PLGA NGC (Figure 7(a)) and SF-PLGA (2:8) NGC (Figure 7(c)) under a microscope camera at 12 weeks after implantation. The regenerated nerves were exposed after removing the PLGA NGC (Figure 7(b)) and SF-PLGA (2:8) NGC (Figure 7(d)). There was a fissure but no collapse occurred in PLGA NGC or SF-PLGA NGC after 12 weeks of implantation. The regenerated nerve was also found after removing the PLGA NGC or SF-PLGA (2:8) NGC.

Electrophysiological evaluation

The electrophysiological examination was performed to evaluate the function of the regenerated nerve, and the values of NCV (Figure 8(a)) and CMAP (Figure 8(b)) were recorded. In the SF-PLGA (2:8) group, the NCV value of the regenerated nerve (45.4 ± 2.4 m/s) was higher than that in the PLGA group (26.9 ± 2.9 m/s), and it was close to that of autograft group (49.5 ± 1.3 m/s). In the SF-PLGA (2:8) group, the CMAP value of the regenerated nerve (12.65 ± 1.12 mV) approximated that of the autograft group (13.7 ± 1.13 mV), which was greater than that in the PLGA group (8.26 ± 1.36 mV). In conclusion, the functional recovery of the regenerated nerve in the SF-PLGA (2:8) group approximated that of the autograft group, which was significantly better than that in the PLGA group ($p < 0.05$).

Histological and histomorphometric analysis

The regenerated nerve was stained with 1% toluidine blue and the transverse section was observed in Figure 9. The regenerated nerve fibers (Figure 9(b)) in the SF-PLGA (2:8) group were more than

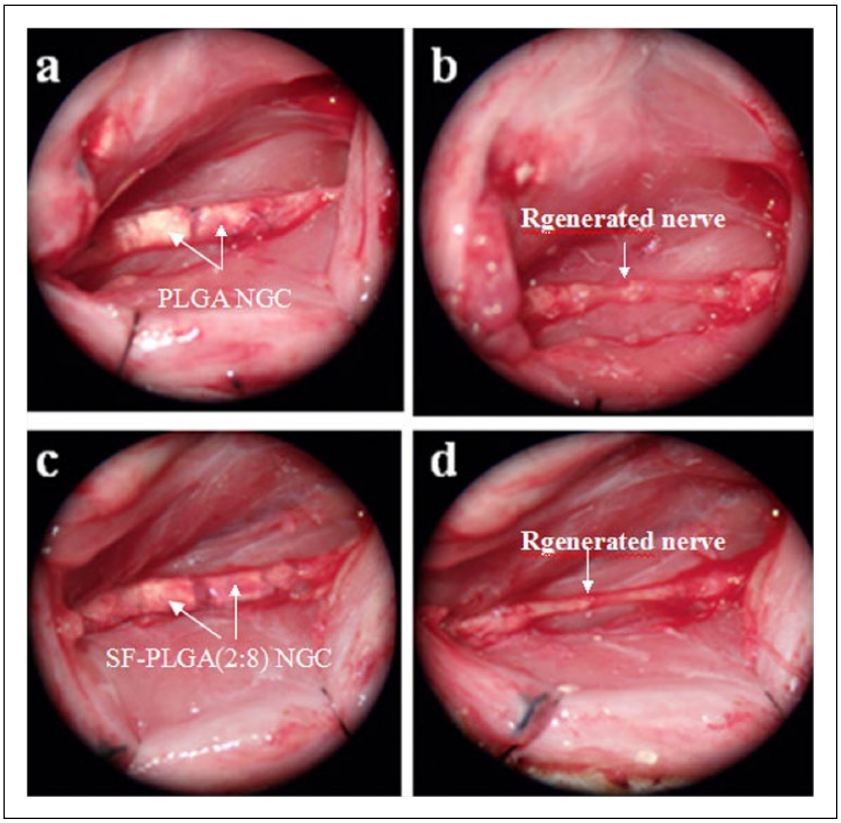

Figure 7. The contour of NGC and regenerated nerve at 12 weeks after implantation under a microscope camera (10×): (a) PLGA NGC, (b) the regenerated nerve after taking away the PLGA NGC, (c) SF-PLGA (2:8) NGC, and (d) the regenerated nerve after taking away the SF-PLGA (2:8) NGC.

that in the PLGA group (Figure 9(a)), which was close to the autograft group (Figure 9(c)). Besides, the distribution of the regenerated nerve fibers in the SF-PLGA (2:8) and autograft groups was more "organized" than that in the PLGA group.

Figure 10(a) shows the number of regenerated nerve fibers in the transverse sections of the three groups. It was observed that the number of regenerated nerve fibers in the SF-PLGA (2:8) group (10,758 ± 975) approximated that of the autograft group (12,288 ± 455), which was significantly larger than that in the PLGA group (5920 ± 339; $p < 0.05$). The maturity of the regenerated nerve was also expressed by the percent neural tissue.[36] Figure 10(b) shows that the percent neural tissue in SF-PLGA (2:8) group (41.2%) was not significantly different with that in the autograft group (42.1%; $p > 0.05$), which was significantly higher than that in the PLGA group (31%; $p < 0.05$).

TEM

Ultrathin sections were also observed under TEM (Figure 11). The maturity of nerve fibers is proportional to the thickness of the myelin sheath. As shown in Figure 11, myelinated axons were surrounded by thick and dark myelin sheath within the nerve specimens (Figure 11(a) to (c)). It was also observed that the thickness of myelin sheath in the SF-PLGA group, PLGA group, and autograft group was 0.37 ± 0.07, 0.26 ± 0.03, and 0.52 ± 0.15 μm, respectively (Figure 11(d)). As for the

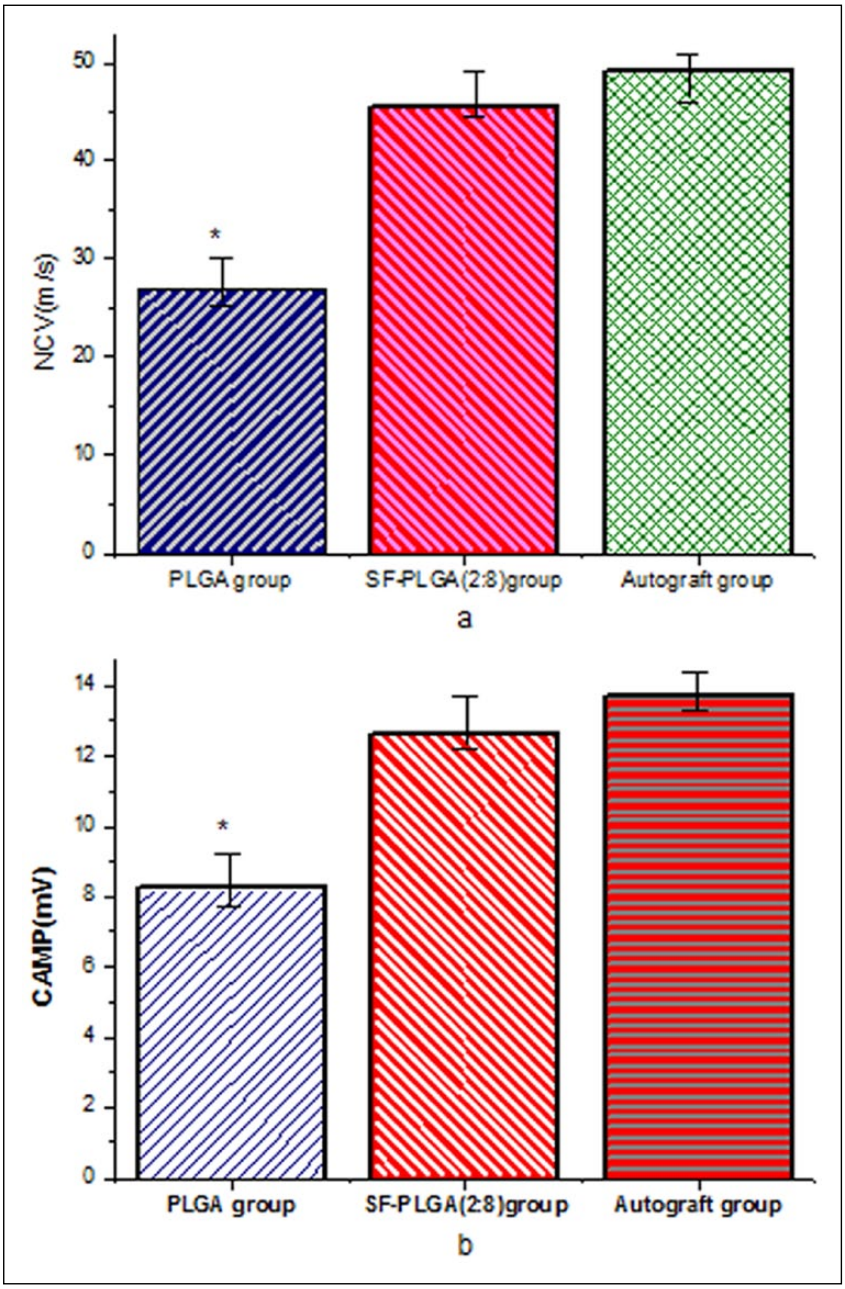

Figure 8. Electrophysiological examination of the regenerated nerve at 12 weeks after implantation: (a) NCV evaluation and (b) CMAP evaluation ($n = 6$; $^*p < 0.05$).

maturity of the regenerated nerve, the SF-PLGA (2:8) group was significantly bigger than the PLGA group. At the same time, we also found that the autograft group was the best among the three groups.

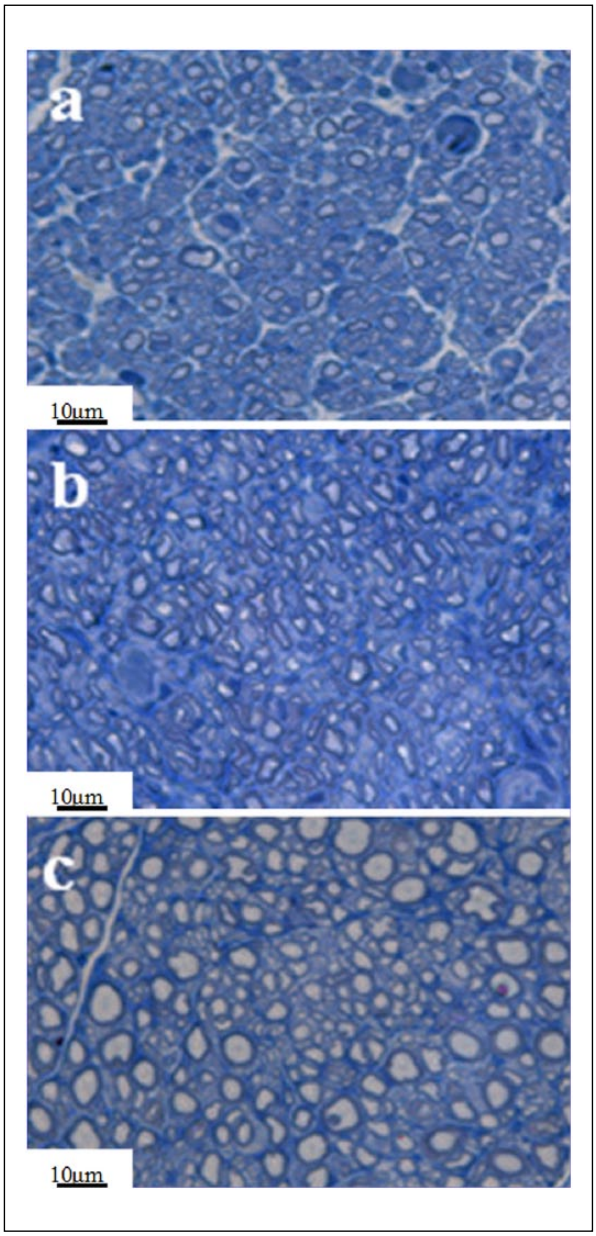

Figure 9. Microanatomy of transverse sections of regenerated nerve specimens stained with 1% toluidine blue: (a) PLGA group, (b) SF-PLGA (2:8) group, and (c) autograft group.

Conclusion

In summary, the SF-PLGA fibrous membrane and the SF-PLGA NGC were prepared via electrospinning with different weight ratios for SF to PLGA. The results showed that the mechanical properties of SF fibrous membrane were improved with the addition PLGA ingredient. While the

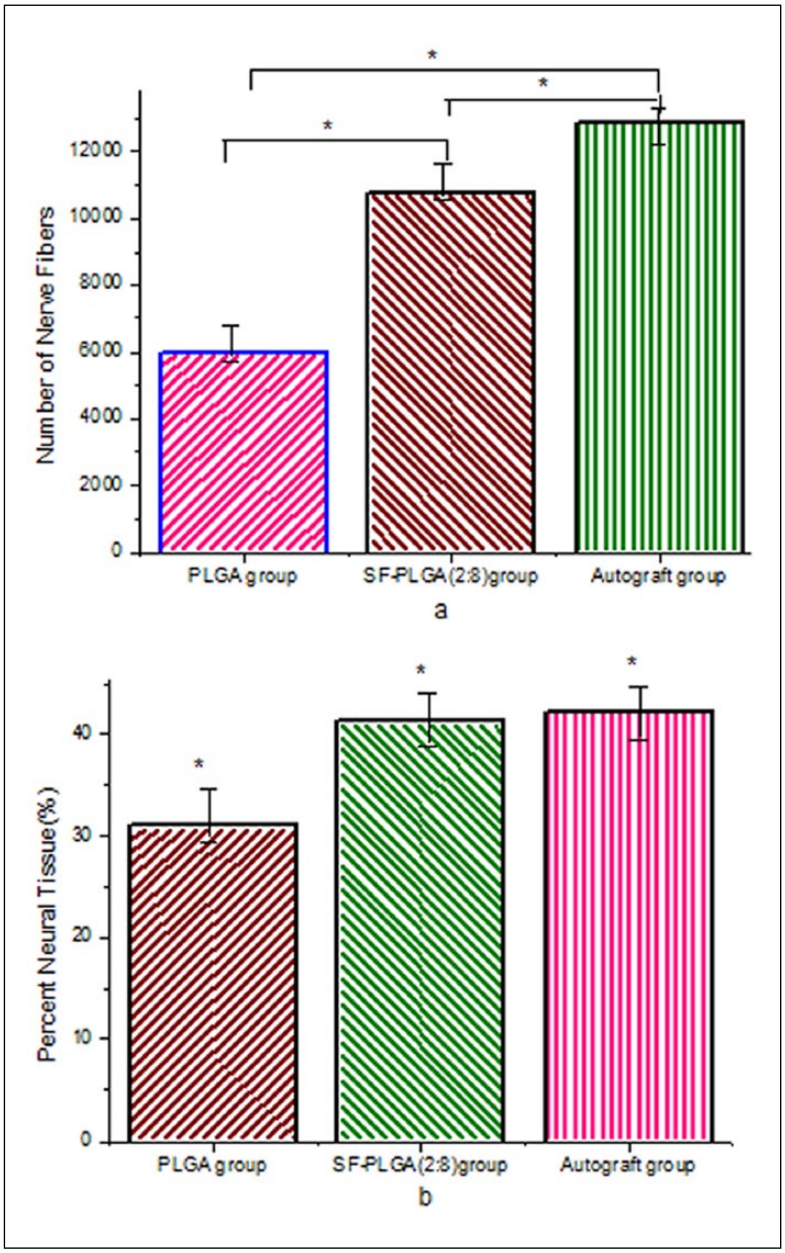

Figure 10. Number of regenerated nerve fibers and percent neural tissue: (a) regenerated nerve fibers in the transverse sections of the three groups and (b) the percent neural tissue in the transverse sections of the three groups ($n = 6$; $^*p < 0.05$).

cell viability on SF-PLGA fibrous membrane was much better than on SF fibrous membrane and PLGA fibrous membrane, especially for the SF-PLGA (2:8) fibrous membrane which showed the highest cell proliferation speed. The degradation rate of the fibrous membrane varied with different weight ratios for SF to PLGA and the SF-PLGA (2:8) fibrous membrane had the highest

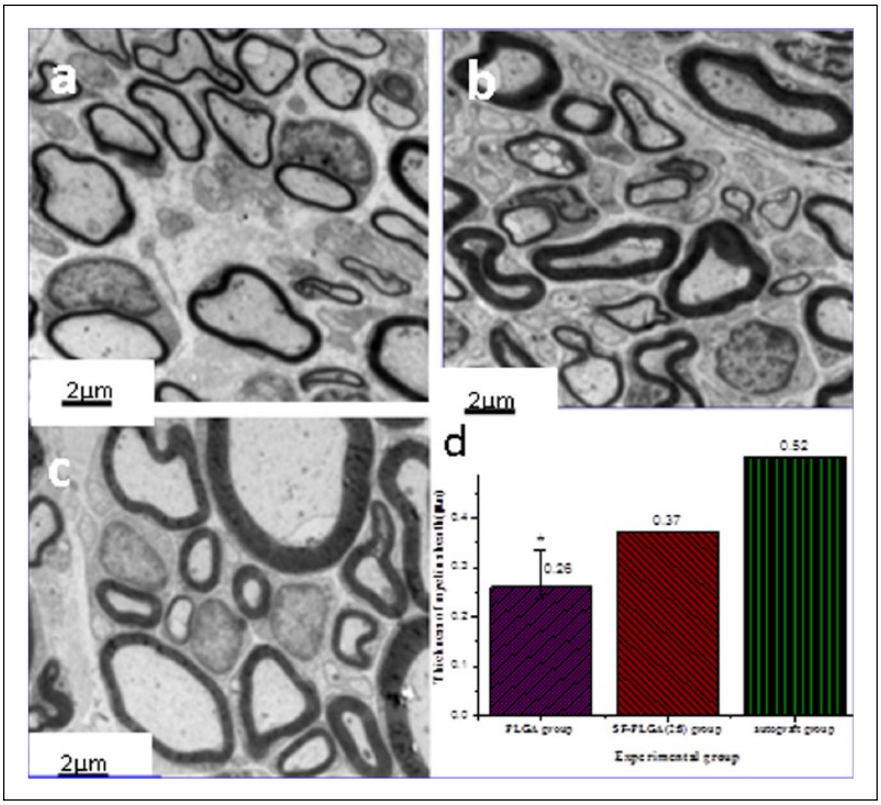

Figure 11. TEM for the regenerated nerve 12 weeks after nerve grafting: (a) PLGA group, (b) SF-PLGA (2:8) group, (c) autograft group, and (d) the myelin sheath thickness of each group ($n = 6$; $^*p < 0.05$).

degradation rate. The results also showed that there was a fissure but no collapse occurred in PLGA NGC or SF-PLGA NGC after 12 weeks of implantation. The regenerated nerve in SF-PLGA (2:8) NGC was more organized and mature than that in PLGA NGC group. This study suggests that the SF-PLGA (2:8) NGC has great potential applications in nerve regeneration.

Declaration of Conflicting Interests

The author(s) declared no potential conflicts of interest with respect to the research, authorship, and/or publication of this article.

Funding

The author(s) disclosed receipt of the following financial support for the research, authorship, and/or publication of this article: This work was financially supported by the National Natural Science Foundation of China (31470941, 31271035), Science and Technology Commission of Shanghai Municipality Program (15JC149010, 15441905100), Research grant no. PGR-VPP-089, Technology Bureau of Jiaxing City (MTC2012-006, 2011A Y1026), Science and Technology Agency of Zhejiang Province (2012R10012-09, 2010R50012-19), and Ph.D. Programs Foundation of Ministry of Education of China (20130075110005) and light of textile project (J201404). The authors would like to extend their sincere appreciation to the Deanship of Scientific Research at King Saud University for its fumding of this research through the research group project no. RGP-201.

References

1. Langer R and Vacanti JP. Tissue engineering. *Science* 1993; 260: 920–926.
2. Chiono V, Ciardelli G, Vozzi G, et al. Enzymatically-modified melt-extruded guides for peripheral nerve repair. *Eng Life Sci* 2008; 8: 226–237.
3. Ruiter GCD, Spinner RJ, Malessy MJ, et al. Accuracy of motor axon regeneration across autograft, single-lumen, and multichannel poly(lactic-co-glycolic acid) nerve tubes. *Neurosurgery* 2008; 63: 144–153.
4. Matsumoto K, Ohnishi K, Kiyotani T, et al. Peripheral nerve regeneration across an 80-mm gap bridged by a polyglycolic acid (PGA)-collagen tube filled with laminin-coated collagen fibers: a histological and electrophysiological evaluation of regenerated nerves. *Brain Res* 2000; 868: 315–328.
5. Huang W, Begum R, Barber T, et al. Regenerative potential of silk conduits in repair of peripheral nerve injury in adult rats. *Biomaterials* 2012; 33: 59–71.
6. Fan WM, Gu J, Hu W, et al. Repairing a 35-mm-long median nerve defect with a chitosan/PGA artificial nerve graft in the human: a case study. *Microsurgery* 2008; 28: 238–242.
7. Ao Q, Wang AJ, Cao WL, et al. Manufacture of multimicrotubule chitosan nerve conduits with novel molds and characterization in vitro. *J Biomed Mater Res A* 2006; 77: 11–18.
8. Stevens MM and George JH. Exploring and engineering the cell surface interface. *Science* 2005; 310: 1135–1138.
9. Yang F, Murugan R, Wang S, et al. Electrospinning of nano/micro scale poly(L-lactic acid) aligned fibers and their potential in neural tissue engineering. *Biomaterials* 2005; 26: 2603–2610.
10. Ghasemi-Mobarakeh L, Prabhakaran MP, Morshed M, et al. Electrospun poly(epsilon-caprolactone)/gelatin nanofibrous scaffolds for nerve tissue engineering. *Biomaterials* 2008; 29: 4532–4539.
11. Chew SY, Mi R, Hoke A, et al. The effect of the alignment of electrospun fibrous scaffolds on Schwann cell maturation. *Biomaterials* 2008; 29: 653–661.
12. Sill TJ and Von Recum HA. Electrospinning: applications in drug delivery and tissue engineering. *Biomaterials* 2008; 29: 1989–2006.
13. Khadka DB and Haynie DT. Insoluble synthetic polypeptide mats from aqueous solution by electrospinning. *ACS Appl Mater Interfaces* 2010; 2: 2728–2732.
14. Wang CY, Zhang KH, Fan CY, et al. Aligned natural-synthetic polyblend nanofibers for peripheral nerve regeneration. *Acta Biomater* 2011; 7: 634–643.
15. Murphy AR, John PS and Kaplan DL. Modification of silk fibroin using diazonium coupling chemistry and the effects on hMSC proliferation and differentiation. *Biomaterials* 2008; 29: 2829–2838.
16. Meinel L, Hofmann S, Karageorgiou V, et al. The inflammatory responses to silk films in vitro and in vivo. *Biomaterials* 2005; 26: 147–155.
17. Kim KH, Jeonge L, Parka HN, et al. Biological efficacy of silk fibroin nanofiber membranes for guided bone regeneration. *J Biotechnol* 2005; 120: 327–339.
18. Min BM, Lee G, Kim SH, et al. Electrospinning of Silk Fibroin nanofibers and its effect on the adhesion and spreading of normal human keratinocytes and fibroblasts in vitro. *Biomaterials* 2004; 25: 1289–1297.
19. Yang YM, Ding F, Wu J, et al. Development and evaluation of silk fibroin-based nerve grafts used for peripheral nerve regeneration. *Biomaterials* 2007; 28: 5526–5535.
20. Yang YM, Chen XM, Ding F, et al. Biocompatibility evaluation of silk fibroin with peripheral nerve tissues and cells in vitro. *Biomaterials* 2007; 28: 1643–1652.
21. Zhang KH, Wang HS, He CL, et al. Fabrication of silk fibroin blended P(LLA-CL) nanofibrous scaffolds for tissue engineering. *J Biomed Mater Res A* 2010; 93: 984–993.
22. Zhang KH, Yin AL, Huang C, et al. Degradation of electrospun SF/P(LLA-CL) blended nanofibrous scaffolds in vitro. *Polym Degrad Stab* 2011; 96: 2266–2275.
23. Zhang KH, Qian YF, Wang HS, et al. Electrospun silk fibroin-hydroxybutyl chitosan nanofibrous scaffolds to biomimic extracellular matrix. *J Biomater Sci Polym Ed* 2011; 22: 1069–1082.
24. Meng ZX, Li HF, Sun ZZ, et al. Fabrication of mineralized electrospun PLGA and PLGA/gelatin nanofibers and their potential in bone tissue

engineering. *Mater Sci Eng C Mater Biol Appl* 2013; 33: 699–706.
25. Wang CY, Liu JJ, Fan CY, et al. The effect of aligned core-shell nanofibres delivering NGF on the promotion of sciatic nerve regeneration. *J Biomater Sci Polym Ed* 2012; 23: 167–184.
26. Wang GL, Hu XD, Lin W, et al. Electrospun PLGA-silk fibroin-collagen nanofibrous scaffolds for nerve tissue engineering. *In Vitro Cell Dev Biol Anim* 2011; 47: 234–240.
27. Meng ZX, Wang YS, Ma C, et al. Electrospinning of PLGA/gelatin randomly-oriented and aligned nanofibers as potential scaffold in tissue engineering. *Mater Sci Eng C Mater Biol Appl* 2010; 30: 1204–1210.
28. Zhang N, Yan HH and Wen XJ. Tissue-engineering approaches for axonal guidance. *Brain Res Rev* 2005; 49: 48–64.
29. Tang X, Xue CB, Wang YX, et al. Bridging peripheral nerve defects with a tissue engineered nerve graft composed of an in vitro cultured nerve equivalent and a silk fibroin-based scaffold. *Biomaterials* 2012; 33: 3860–3867.
30. Gonsalves KE, Chen X and Cameron JA. Degradation of nonalternating poly(ester amides). *Macromolecules* 1992; 25: 3309–3312.
31. Zhang XF, Coughlan A, O'Shea H, et al. Experimental composite guidance conduits for peripheral nerve repair: an evaluation of ion release. *Mater Sci Eng C Mater Biol Appl* 2012; 32: 1654–1663.
32. Loo JS, Ooi CP and Boey FY. Degradation of poly(lactide-co-glycolide) (PLGA) and poly(L-lactide) (PLLA) by electron beam radiation. *Biomaterials* 2005; 26: 1359–1367.
33. Liu H, Wang SD and Qi N. Controllable structure, properties, and degradation of the electrospun PLGA/PLA-blended nanofibrous scaffolds. *J Appl Polym Sci* 2012; 125: 468–475.
34. Kehoe S, Zhang XF, Lewis L, et al. Characterization of PLGA based composite nerve guidance conduits: effect of F127 content on modulus over time in simulated physiological conditions. *J Mech Behav Biomed Mater* 2012; 14: 180–185.
35. Campillo-Fernández AJ, Unger RE, Peters K, et al. Analysis of the biological response of endothelial and fibroblast cells cultured on synthetic scaffolds with various hydrophilic/hydrophobic ratios: influence of fibronectin adsorption and conformation. *Tissue Eng Part A* 2009; 15: 1331–1341.
36. Itoh S, Takakuda K, Ichinose S, et al. A study of induction of nerve regeneration using bioabsorbable tubes. *J Reconstr Microsurg* 2001; 17: 115–123.